KFKI-1988-64/D

S. ZOLETNIK

PERIODIC DISRUPTIONS IN THE MT-1 TOKAMAK

Hungarian Academy of Sciences

CENTRAL
RESEARCH
INSTITUTE FOR
PHYSICS

BUDAPEST

KFKI-1988-64/D
PREPRINT

PERIODIC DISRUPTIONS IN THE MT-1 TOKAMAK

S. ZOLETNIK

Central Research Institute for Physics
H-1525 Budapest 114, P.O.B.49, Hungary

HU ISSN 0368 5330

S. Zoletnik: Periodic disruption in the MT-1 tokamak. KFKI-1988-64/D

ABSTRACT

Periodic minor disruptions were measured in the MT-1 tokamak with the limiter safety factor value between 4 and 10. The density limit as a function of plasma current and horizontal displacement was investigated. Precursor oscillations of mode numbers m = 2/n = 1 always appear before the instability with increasing amplitude but can be observed at the density limit with quasi-stationary amplitude too. Phase correlation between precursor oscillations measured by Mirnov coils and soft X-ray detectors show good agreement with a simple magnetic island model and reveal that the assumed island is located deep inside the plasma.

Ш. Золетник: Периодические неустойчивости срыва на токамаке МТ-1. KFKI-1988-64/D

АННОТАЦИЯ

На токамаке МТ-1 с запасом устойчивости 4-10 были измерены периодические неустойчивости срыва. Изучался предел плотности электронов в зависимости от тока и горизонтального положения плазменного шнура. Колебания моды m = 2, n = 1 появлялись всегда перед неустойчивостью, а их можно было наблюдать при предельной плотности со стационарной амплитудой. Корреляции фаз между колебаниями, измеренные различными зондами Мирнова и детекторами мягкого рентгеновского излучения показывают хорошее согласие с результатами модели магнитных островов. Эти данные доказывают, что предположенные острова лежат глубоко в плазме.

Zoletnik S.: Periodikus diszrupciók az MT-1 tokamakban. KFKI-1988-64/D

KIVONAT

Periodikus diszrupciókat mértünk az MT-1 tokamakon a 4-10 q_a értéktartományban. Vizsgáltuk a diszrupciós sűrűség határt a plazmaáram és a plazma vízszintes elmozdulásának függvényében. Az instabilitások előtt gyorsan növekvő amplitudóju m = 2/n = 1 módusú precursor rezgések jelentek meg, de a diszrupciós határnál közel állandó amplitudóval is mérhetők voltak. A különböző Mirnov szondákkal és lágy röntgen detektorokkal mért precursor rezgések relatív fázisai jó egyezést mutattak egy egyszerű forgó mágneses sziget modellel, és feltárták, hogy a sziget mélyén a plazma belsejében helyezkedik el.

1. Introduction

Disruptive instabilities are common phencmena in toroidal devices, especially in tokamaks. In the Kadomtsev classification [1] 3 main types are distinguished: internal, minor, and major disruptions. This paper deals with the systematic investigation of periodic minor disruptions in the MT–1 tokamak ($R = 0.4m$, $a = 0.09m$, $B_t \leq 1.2T$, $I_p = 8 - 40kA$). All the measurements were performed at $B_t = 1T$ using a 9 cm aperture limiter. The MT–1 tokamak is enclosed in a $2cm$ thick copper shell located at $r = 12cm$. From the conductivity and the electron temperature, calculated from the soft X–ray spectrum, Z_{eff} is estimated to be 3–5. During the experiments the following diagnostics were used: plasma current and loop voltage measuring coils, 17 Mirnov coils for plasma position and magnetic field fluctuation, 2 mm microwave interferometer for electron density measurement, 5 chord soft X-ray camera, 5 channel neutral particle analyser.

Periodic minor disruptions have been reported in various tokamaks [2-4]. In the MT–1 machine disruption–like periodic instabilities have been seen for a long time [5]. Such disruptions can be well reproduced without causing damage to the tokamak. In the first part of this paper various features of the instability are, be summarized; in subsequent parts the density limit and precursor oscillations will be examined.

2.1 Characteristics of the instability

In *Fig. 1* typical diagnostic signals are shown during a shot with periodic instabilities. It can be seen that during the instabilities fast current jumps and large negative loop voltage spikes occur. In the MT–1 tokamak there is no control of the plasma current, so these current spikes can be produced inductively by rearrangement of the radial current distribution.

After the first disruption the plasma goes to a higher average resistivity state, which is shown by the higher average loop voltage value. Between the large current jumps smaller quasi-periodic ones can be seen. The large peaks follow the periodicity of the smaller ones. Detailed investigations have shown that the small instabilities have the same features as the large ones. These instability groups are always present in a wide range of parameter space.

At the onset of the disruptions the soft X-ray emission along the central chord abruptly decreases (*Fig. 1/c*), whereas it increases in the outer chords. The inversion radius for this process (not for the internal disruptions) was found to be approximately 3–4 cm in 20 kA discharges, and less than 3 cm for 10 kA discharges. The width of the radial soft X–ray emission distribution, measured by the five chord camera increases during the fast current rise (*Fig. 1/e*). As no characteristic change was shown on the electron density signal, the X-ray emission redistribution must have been caused mainly by a change in the electron temperature distribution.

The horizontal plasma position in *Fig. 1/d* measured by Mirnov coils [6] shows fast inward jumps in major radius correlated with the current rise. This feature was seen by the vertical soft X-ray camera too.

In *Fig. 2/b* the neutral hydrogen atom emission signal is shown in one energy window. (integrating time constant $100\mu s$). *Fig. 2/a* shows the current signal for the same discharge. The starting points of the peaks in the neutral particle emission show a characteristic $20-40\mu s$ time delay relative to the current peak starting points.

2.2 Disruptive regimes in the parameter space of the MT-1 tokamak.

Initial examination of the periodic disruptions showed that the instability occurs at high densities [5] and/or if the plasma is displaced from the center of the vacuum vessel. Z_{eff} may have a significant role in determining the disruptive regimes, but as no reliable measurement is performed on this parameter an effort was made to minimize the effects of changing Z_{eff}. All measurement series were started under similar vacuum conditions after the baking of the liner. Within one series of measurements no systematic change of the density limit was detected.

In order to find unstable regimes in the operating space a data set consisting of 121 disruptive shots was created and analysed. Three parameters were calculated just before the first disruption of a discharge, *viz.* plasma current, line density, and horizontal displacement.

Fig. 3 shows a Hugill plot for well centered discharges, where linear dependence of the normalized electron density *vs.* $1/q_a$, for high q discharges [1,7], is clearly seen — though the slope of the line is about 2 times higher than that of Ref. [1].

In *Fig. 4*, $\bar{n}_e$ values are shown *vs.* horizontal displacement for three different current ranges. A clear trend can be seen which lowers the disruptive density limit at higher displacement values. The density limit decrease is more definite for higher currents.

2.3 Precursor oscillations

Precursor oscillations before disruptions are always seen in the MT-1 tokamak. In most cases these appear for only a short time (3-5 periods) before the instability. If the electron density changes slowly ($\approx 2\ 10^{18} m^{-3}/ms$), precursor oscillations with quasi-stationary amplitude appear at about 70–80% of the density at the disruption. Usually sawtooth-like modulation is observed on the precursor amplitude (*Fig. 5/a*). When the amplitude drops, similar but much smaller changes can be seen in the diagnostic signals than in the case of the disruption. In *Fig. 5* a series of such events is shown. The loop voltage produces negative peaks, the central soft X-ray emission drops, the width of the soft X-ray distribution increases and the plasma moves inwards. This quasi-stationary precursor phase is usually terminated by a disruption, the precursor oscillation of which is evolves from the quasi-stationary ones. No frequency or phase shift change precedes the disruption.

Fast Fourier frequency analysis showed one main peak in the *amplitude* spectrum of the precursor oscillations and usually about 10 % second harmonic amplitude. Other frequencies never appeared in the picture. A method has been developed for calculating the frequency and phase changes of the precursor oscillations with approximately one period time resolution. Neither before disruptions nor during the events shown in *Fig 5* have systematic changes in frequency and/or in phase shifts been observed. By means of Mirnov coils located at different poloidal and toroidal angles the mode numbers were measured. In every case they turned out to be $m = 2$, $n = 1$. In the poloidal cross section the perturbation rotated in the electron diamagnetic direction. The helicity of the perturbation followed the magnetic field lines.

Assuming that the precursor oscillations are caused by a rotating 2/1 magnetic island an attempt was made to measure its radial position. For this purpose the 5 channel soft X–ray detector array was used. The oscillations were clearly seen on the signals of the detectors so one could measure their relative phases and amplitudes.

In order to simplify the situation the simple assumption was used that the magnetic island flattens the soft X-ray emission profile inside its separatrix [3,8]. The poloidal cross section of the magnetic surfaces of such an island is shown in *Fig. 6* for an analytically given 2/1 current perturbation. If the detectors look through a rotating structure like this, they see sinusoidal fluctuations. Using only the first harmonic of these, one is able to calculate numerically the phases and amplitudes of the oscillations as a function of 4 parameters of the magnetic island. These were the following (see *Fig. 6*):

d : horizontal displacement of the island chain relative to the vessel centre,

r_0 : radius of the island chain,

w : width of the island chain.

a : the width of the equilibrium soft X–ray intensity distribution,

The calculated phase shifts for a multi detector soft X-ray camera resemble the measured ones given in ref. [9]. The typical double phase reversal of it is measured on the MT-1 tokamak too by the 5 detector array. With a simplex method [11] we numerically fitted the four parameters to the measured phase and amplitude values. An approximate error analysis of the results showed that the 5 detectors are insufficient for calculating the island width (w), but the island chain radius and the horizontal displacement is well determined. Parameter a depends on the actual equilibrium radial distribution which is unknown.

The r_0 parameter of the perturbation (island chain radius) for 20 kA shots turned out to be approx. 5 cm. For lower currents the oscillations could be seen only in the central 3 detectors so it was impossible to calculate the island parameters.

The model island of *Fig 6* was used for calculating the relative phases between Mirnov coil and soft X-ray oscillations. The current maxima of this islands are at the x points, so the soft X-ray perturbation maxima are rotated 90° relative to the current maxima. Mirnov coil – soft X-ray oscillation relative phases were calculated on this basis and they are in good agreement (within 20°) with the calculated ones.

3. Conclusions

Periodic disruptions have been measured in the MT-1 tokamak. Diagnostic signals show similar characteristics to those of density limit disruptions on other tokamaks, namely: fast current jump, negative voltage spike, inward jump in major radius, widening of plasma column in minor radius, 2/1 precursor oscillations, cooling of the plasma at the instability. Disruptions become non-periodic if $q_a \leq 3.5$, which may be caused by the $q = 2$ surface approaching the limiter.

The density limit of these disruptions was examined as a function of plasma current and horizontal displacement. When the plasma is maintained in the centre of the vacuum vessel the usual linear dependence of $1/q_a$ on the normalized density can be seen on the Hugill plot but the slope of the line is about twice that of given in Ref. [1] for q_a values above 3.5. When the plasma is displaced from the centre, the density limit decreases. The decrease is pronounced at higher currents. This behaviour cannot be understood on the basis of the Hugill plot because when the plasma is shifted from the centre, the effective minor radius becomes smaller thereby decreasing the effective q_a. This would cause a higher density limit if q_a stays above 3.5, but actually the density limit decreases. This degradation is possibly caused by the non axisymmetric plasma profile.

Measurements of precursor oscillations showed the presence of a 2/1 magnetic island, though others (e. g. the 3/2 mode [8]) cannot be ruled out because of the low resolution of the soft X-ray camera. The radius of the island is estimated to be about 5 cm for 20 kA discharges. To compare this with the radius of the $q = 2$ surface the latter was estimated using the following procedure. Internal disruptions usually appear above 20 kA plasma current which means $q_0 \approx 1$. From this, parameter ν of a $j(r) = j_0(1 - r^2/a^2)^\nu$ parametric current distribution can be calculated which gives $r_{q=2} = 5.4cm$. The inversion radius for the periodic disruptions is much less ($\approx 3.5cm$) than both the island radius and the $q = 2$ radius. This fact is in contrast with Refs. [4] and [10] where $r_{inv} \approx r_{q=2}$, but resembles the case of Ref. [8] where this kind of disruption is considered to be caused by the interaction of the 2/1 mode with the 1/1 or 3/2 mode.

ACKNOWLEDGEMENTS

The author is grateful to Dr. A. Montvai, who initiated this subject, for helpful discussions during the whole work. He would also like to thank the whole MT-1 group for support and Dr. G. Petravich for the neutral particle emisson measurements.

REFERENCES

[1] KADOMTSEV, B.B., Plasma Physics and Controlled Fusion 26 1A (1984) 217.

[2] GORBUNOV, E.P., RAZUMOVA, K.A., At. ehnerg. 15 (1963) 363.

[3] TURNER, M.F., WESSON, J.A., Nuclear Fusion 22 (1982) 1069.

[4] CASTRACANE, J., MOOS, H.V., RICE, J.E., Physics Letters 88A (1982) 295.

[5] MONTVAI, A., PÓCS, L., VÁLYI, L., ZOLETNIK, S., in Controlled Fusion and Plasma Physics (Proc. EPS XI. Fusion Conf. Aachen, 1983), Vol. 7D, Part I., 119.

[6] ZOLETNIK, S., MONTVAI, A., Determination of the Centre of Gravity of the Current Distribution in the MT 1 Tokamak., Central Research Inst. for Phys. report KFKI-1986-10/D (1986).

[7] NIEDERMEYER, H., BARTIMORO, R., BECKER, G., in Controlled Fusion and Plasma Physics (Proc. EPS XII. Fusion Conf. Budapest, 1985), Vol. 9F, Part I., 159.

[8] TSUJI, S., NAGAYAMA, Y., MIYAMOTO, K., Nuclear Fusion 25 (1985) 305.

[9] SAUTHOFF, N.R., von GOELER, S., STODIEK, W., Nuclear Fusion 18 (1978) 1445.

[10] von GOELER, S., X-ray measurements on the ST tokamak, Proc. EPS VII. Fusion Conf. Lausanne, 1975 Vol II. 71.

[11] NELDER, J.A., MEAD, R., Computer J. 13, 317 (1970).

Figure captions

Fig. 1. The most characteristic signals of a disruptive discharge (timescale $1ms/div$).

a/ Plasma current ,

b/ Loop voltage,

c/ Soft X–ray intensity measured by a 5 channel detector array looking vertically into the tokamak,

d/ Horizontal displacement of the plasma column relative to the vessel centre. Dotted horizontal line shows 0, positive values record movement to the outside,

e/ Square of the width of the radial soft X–ray intensity distribution measured by the 5 channel detector array.

Fig. 2. Plasma current and neutral hydrogen atom emission signal for a disruptive discharge (timescale $1ms/div$). Integrating time constant for the H emission curve is $100\mu s$.

Fig. 3. Hugill plot for well centered discharges.

Fig. 4. Line averaged electron density *vs.* horizontal plasma displacement measured just before the first disruption of disruptive discharges for three different current ranges.

Fig. 5. Characteristic diagnostic signals in the case of quasi–stationary precursor oscillations (timescale $200\mu s/div$)

a/ Mirnov coil signal in the horizontal plane at the outer side of the tokamak.

b/ – e/ The same signals as in *Fig. 1.*

Fig. 6. Calculated magnetic surface cross sections for an $m/n = 2/1$ current perturbation. Tokamak centre is to the left.

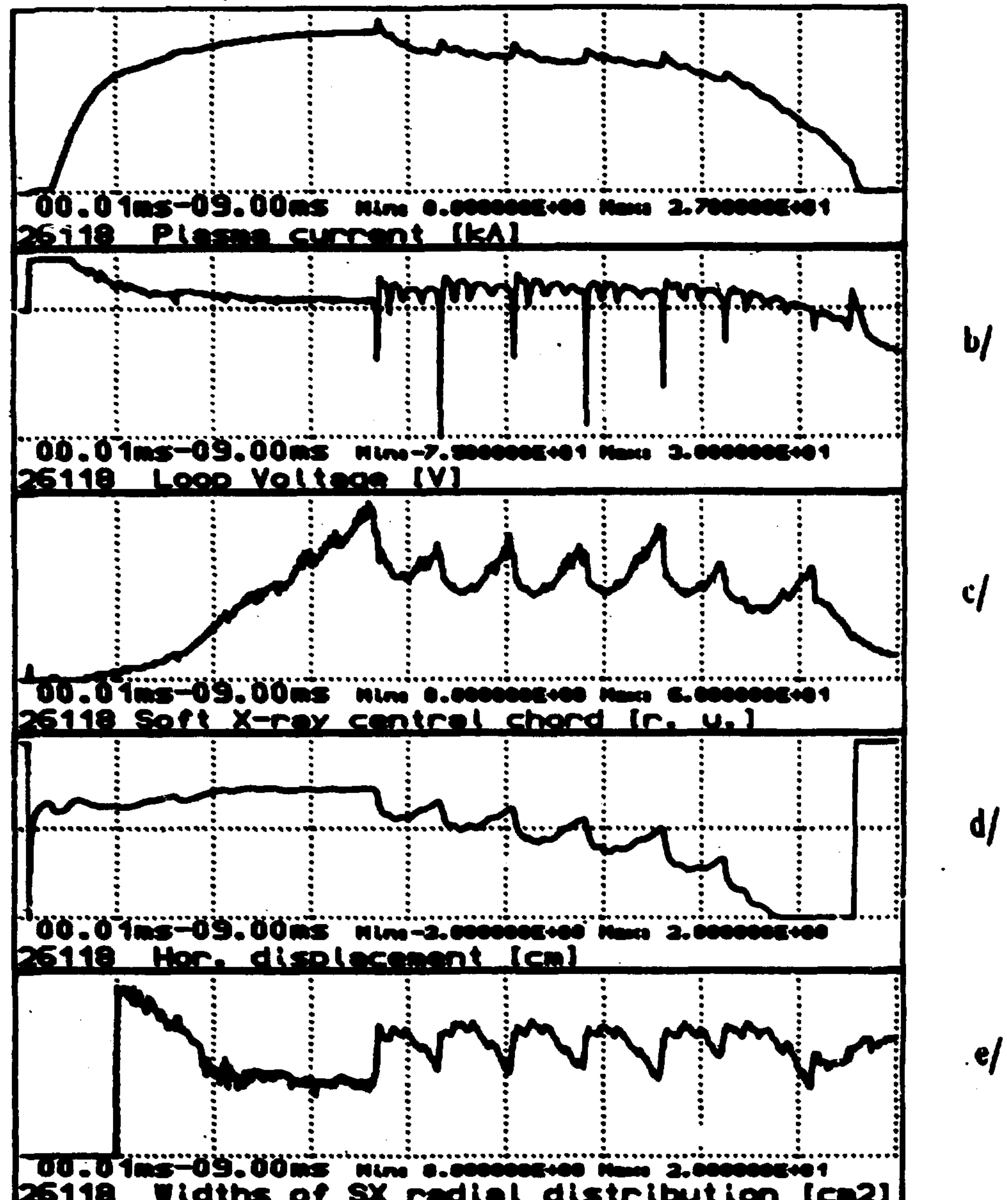
00.01ms-09.00ms Min: 0.000000E+00 Max: 2.700000E+01
26118 Plasma current [kA]
00.01ms-09.00ms Min:-7.500000E+01 Max: 3.000000E+01
26118 Loop Voltage [V]
00.01ms-09.00ms Min: 0.000000E+00 Max: 6.000000E+01
26118 Soft X-ray central chord [r. u.]
00.01ms-09.00ms Min:-2.000000E+00 Max: 2.000000E+00
26118 Hor. displacement [cm]
00.01ms-09.00ms Min: 0.000000E+00 Max: 2.000000E+01
26118 Widths of SX radial distribution [cm2]
b/
c/
d/
e/

Fig. 1.

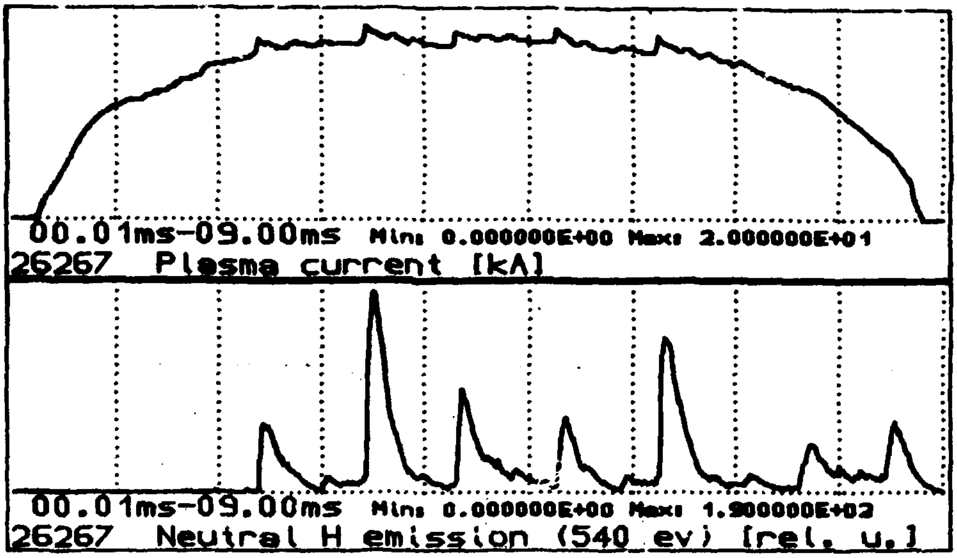
00.01ms-09.00ms Min: 0.000000E+00 Max: 2.000000E+01
26267 Plasma current [kA]
00.01ms-09.00ms Min: 0.000000E+00 Max: 1.900000E+02
26267 Neutral H emission (540 ev) [rel. u.]

Fig. 2.

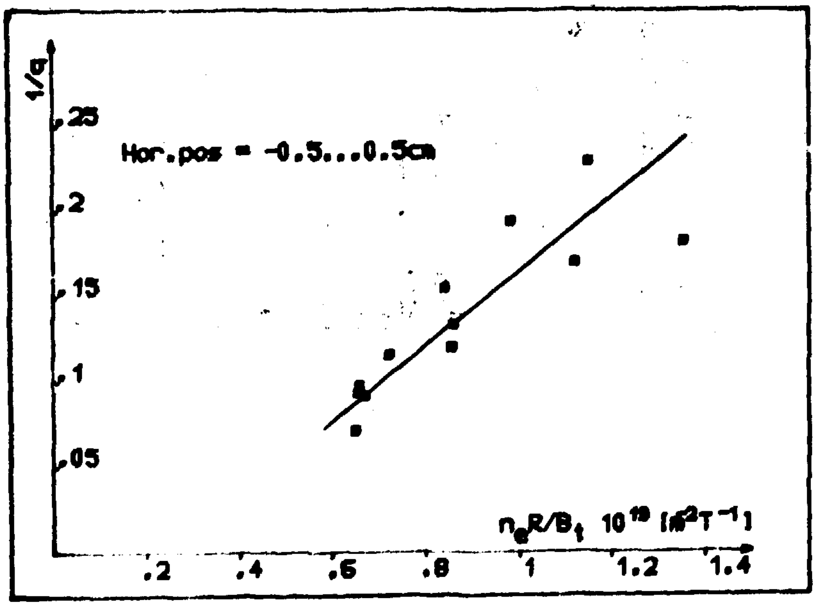
1/q
.25
.2
.15
.1
.05
Hor.pos = -0.5...0.5cm
$n_e R/B_t$ 10^{19} [$m^2 T^{-1}$]
.2
.4
.6
.8
1
1.2
1.4

Fig. 3.

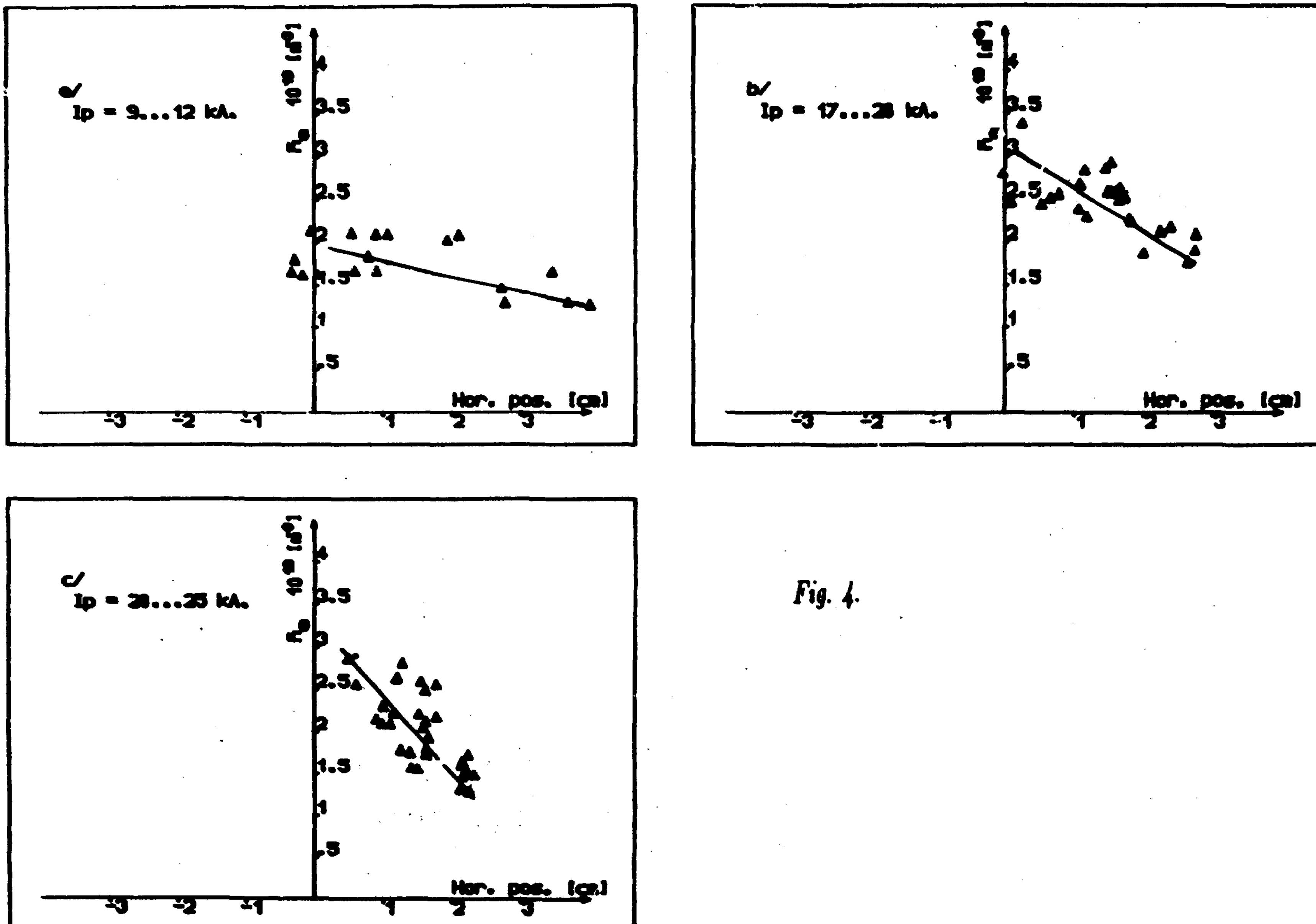
a/
Ip = 9...12 kA.
n_e 10[13] [cm^{-3}]
Hor. pos. [cm]
b/
Ip = 17...28 kA.
n_e 10[13] [cm^{-3}]
Hor. pos. [cm]
c/
Ip = 28...25 kA.
n_e 10[13] [cm^{-3}]
Hor. pos. [cm]

Fig. 4.

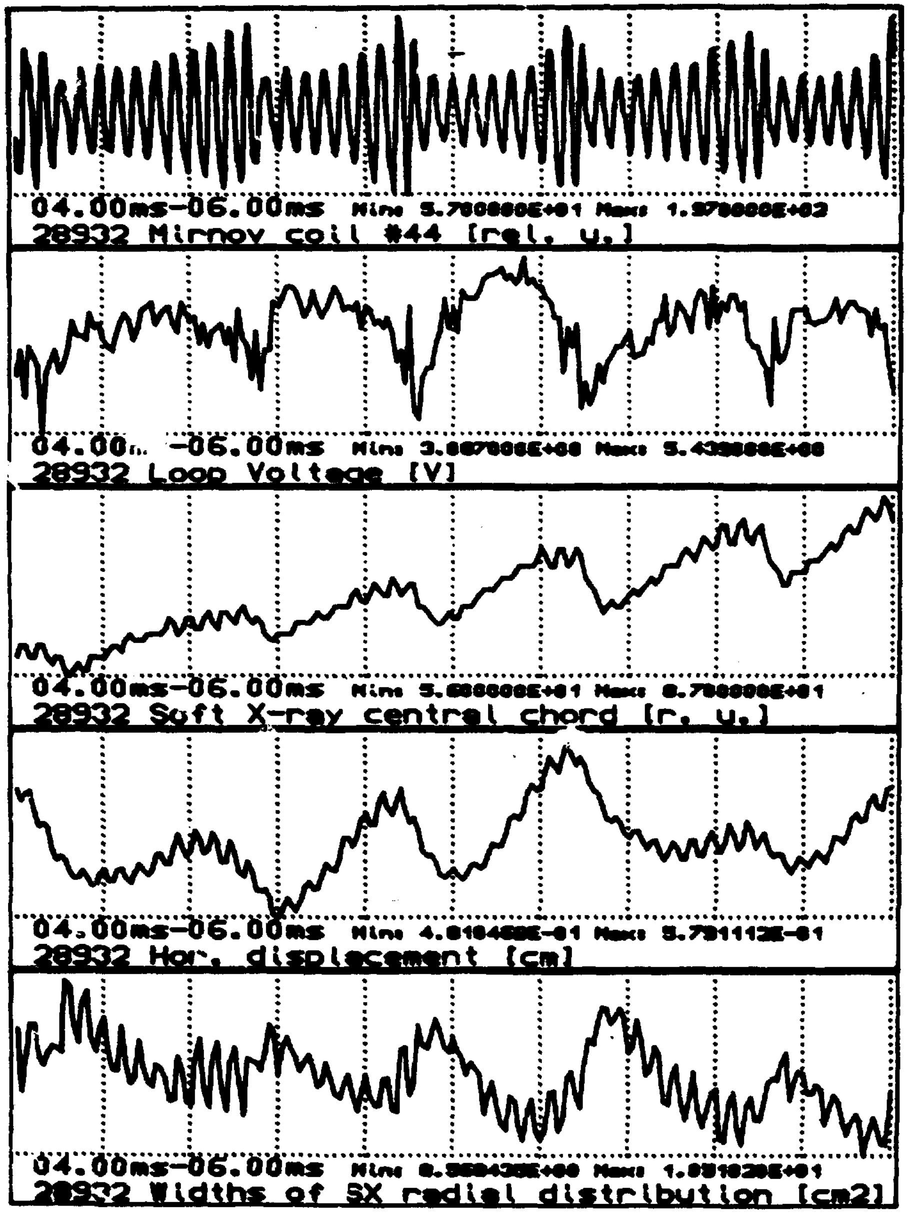
04.00ms-06.00ms
28932 Mirnov coil #44 [rel. u.]
a/
-06.00ms
28932 Loop Voltage [V]
b/
04.00ms-06.00ms
28932 Soft X-ray central chord [r. u.]
c/
04.00ms-06.00ms
28932 Hor. displacement [cm]
d/
04.00ms-06.00ms
28932 Widths of SX radial distribution [cm2]
e/

Fig. 5.

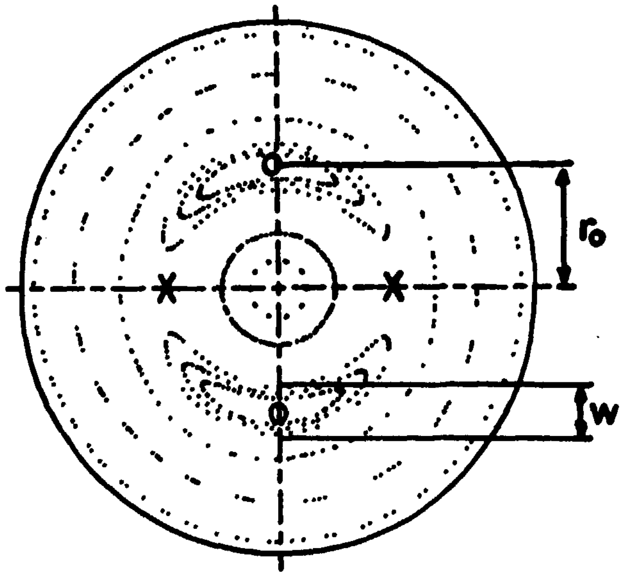

Fig. 6.

The issues of the KFKI preprint/report series are classified as follows:

A. Particle and Nuclear Physics

B. General Relativity and Gravitation

C. Cosmic Rays and Space Research

D. Fusion and Plasma Physics

E. Solid State Physics

F. Semiconductor and Bubble Memory Physics and Technology

G. Nuclear Reactor Physics and Technology

H. Laboratory, Biomedical and Nuclear Reactor Electronics

I. Mechanical, Precision Mechanical and Nuclear Engineering

J. Analytical and Physical Chemistry

K. Health Physics

L. Vibration Analysis, CAD, CAM

M. Hardware and Software Development, Computer Applications, Programming

N. Computer Design, CAMAC, Computer Controlled Measurements

The complete series or issues discussing one or more of the subjects can be ordered; institutions are kindly requested to contact the KFKI Library, individuals the authors.

Title and classification of the issues published this year:

KFKI-1988-01/A L. Diósi	On the motion of solids in modified quantum mechanics
KFKI-1988-02/D Bakos J.	Thermonuclear plasmaphysical research in the Central Research Institute for Physics (1986-1987) (in Hungarian)
KFKI-1988-03/E A. Jákli et al.	A special shear method of alignment for smectic liquid crystals
KFKI-1988-04/A L. Diósi et al.	Restoration of $2-\pi^{0}$ inclusive distribution from observed $2-\gamma$ data
KFKI-1988-05/A L. Diósi	Continuous quantum measurement and Itô formalism
KFKI-1988-06/E G. Konczos et al.	Amorphous alloys bibliography 1984-1987: papers from the Central Research Institute for Physics /Budapest/ and cooperating institutions
KFKI-1988-07/E L. Gránásy et al.	Superconductivity without rear earth metals in pure and Fe dopped Bi-Cu-Sr-Ca oxide systems (in Hungarian)
KFKI-1988-08/B B. Lukács et al.	Galaxy formation from tepid inflation
KFKI-1988-09/E I. Furó et al.	Fluctuating electronic magnetic moment in $YBa_2Cu_3O_{6.2}$: an NMR and NQR study
KFKI-1988-10/M A.K. Sdaa et al.	The analysis of the alternating bit protocols
KFKI-1988-11/M R. Wittmann	Introduction to Milner's Calculus of Communicating Systems
KFKI-1988-12/E A. Rockenbauer et al.	Magnetic field dependent microwave absorption in the multiphase Bi-Sr-Ca-Cu oxide system

KFKI-1988-13/M M. Barbuceanu et al.	XRL: A layered knowledge processing architecture able to enhance itself
KFKI-1988-14/B L. Diósi et al.	Mapping the van der Waals state space
KFKI-1988-15/E L. Mihály et al.	Experimental studies on high temperature superconductors
KFKI-1988-16/M P. Ecsedi-Tóth et al.	The LOTOS specification language /in Hungarian/
KFKI-1988-17/A A. Frenkel	The reduction of the Schrödinger wave function and the emergence of classical behavior
KFKI-1988-18/E N. Kroó et al.	Decay time measurement of surface plasmons on silver gratings
KFKI-1988-19/A P. Hidas	The inclusive production of the Ξ^- particles in 280 GeV/c muon-proton interactions
KFKI-1988-20/A T. Dolinszky et al.	A new class of analytically solvable quantum scattering problems
KFKI-1988-21/A L. Diósi	Localized solution of simple nonlinear quantum Langevin-equation
KFKI-1988-22/E H. Kuzmany et al.	Oxygen induced phase changes in $YBa_2Cu_3O_{6+\delta}$. Transport, structural and spectoscopic evidence
KFKI-1988-23/E K. Tompa et al.	$^{205}T\ell$ NMR spin echo investigations in multiphase $T\ell$-Ba-Ca-Cu oxide superconductors
KFKI-1988-24/G R. Kozma et al.	Experimental study of the field-of-view of neutron detectors towards thermohydraulic perturbances
KFKI-1988-25/K K. Fodor-Csorba et al.	Structure-activity relationship studies on the antidotes of thiocarbamate herbicides /in Russian/
KFKI-1988-26/D D.N. Yundev et al.	Measurement of the absorption coefficient and index of refraction of templene in the submillimetre wave range
KFKI-1988-27/E B. Sas et al.	Thermoelectric power and anisotropic magnetoresistance of Fe-TM-B-amorphous alloys
KFKI-1988-28/M S. Wagner-Dibuz	Protocol consultant, an expert system for protocol engineering
KFKI-1988-29/E L. Rosta	Neutron physical properties of a multidisc velocity selector
KFKI-1988-30/A B. Kämpfer et al.	Anisotropic nuclear matter with momentum-dependent interaction
KFKI-1988-31/E L. Bottyán et al.	Evidence for Fe^{4+} in $YBa_2(Cu_{1-x}M_x)_3O_{7-y}$ ($M={}^{57}Co$, ^{57}Fe) by absorption and emission Mössbauer spectroscopy
KFKI-1988-32/C K. Szegő et al.	Surface and dust features seen on the nucleus of Comet Halley
KFKI-1988-33/C K. Szegő et al.	Dust photometry in the near nucleus region of Comet Halley
KFKI-1988-34/G,M B.K. Szabó	Part-task simulator for a WWER-440 nuclear power plant subsystem

KFKI-1988-35/E P. Jani	Time-interval statistics for laser Doppler anemometry use. (in Hungarian)
KFKI-1988-36/J G. Nowotny et al.	Analytical methods used for determination of heavy water concentration
KFKI-1988-37/M Abdulmagied K. Sdaa	Development and Structure of a DLL with a new DECISION TREE approach for Protocols
KFKI-1988-38/A L. Diósi	Landau's density matrix in quantum-electrodynamics
KFKI-1988-39/B Z. Perjés	Parametric manifolds
KFKI-1988-40/A V.B. Belyaev et al.	Dynamics of the fusion reaction in the $dt\mu^-$ system
KFKI-1988-41/E Z. Gingl et al.	Local structure of icosahedral quasicrystals
KFKI-1988-42/E J. Kollár et al.	Quasiperiodic lattice model in two dimensions
KFKI-1988-43/E P. Jani	Comparison of time interval statistics with auto-correlation date gathering techniques in laser Doppler anemometry (in Hungarian)
KFKI-1988-44/G A. Gács et al.	Instructor support and malfunction handling in the WWER-440 basic principles simulator
KFKI-1988-45/D L. Csillag et al.	Linewidth studies on the 469.4 nm Kr^+ laser transition
KFKI-1988-46/G J.S. Jánosy et al.	Modelling approaches for a basic principles simulator for WWER-440 (PWR) Nuclear Power Plants
KFKI-1988-47/G Gy. Ézsöl et al.	Analysis of consequences of steam generator collector rupture. Plant analysis with the RELAP4/MOD6 code based on PMK-NVH test results. (in Hungarian)
KFKI-1988-48/G L. Szabados et al.	Analysis of consequences of steam generator collector rupture. Computer code analysis and interpretation of PMK-NVH test results. (in Hungarian)
KFKI-1988-49/E Gy. Zsigmond et al.	Cold neutron source at the Budapest WWR-SM reactor (in Hungarian)
KFKI-1988-50/M L. Ungvári	State-oriented analysis of connection establishment phase of the data link control protocol LAPB (in Hungarian)
KFKI-1988-51/E L. Potocký et al.	Metallic glasses cast in magnetic field
KFKI-1988-52/E L. Potocký et al.	Surface coercive force of some metallic glasses
KFKI-1988-53/E D. Huber et al.	Influence of the field induced doping effect on the density of states in highly doped *n*-type *a-Si:H*
KFKI-1988-54/D J.S. Bakos et al.	Tokamak edge plasma investigation by laser blow-off

KFKI-1988-55/A L. Diósi	Models for universal reduction of macroscopic quantum fluctuations
KFKI-1988-56/B B. Lukács	Once more about economic entropy
KFKI-1988-57/A J. Révai	A model for studying time dependent quantum mechanical processes and its application for quasi-stationary states
KFKI-1988-53/M A. Farkas et al.	A short presentation of SSADM (Structured Systems Analysis and Design Method) (in Hungarian)
KFKI-1988-59/A B. Kämpfer	Equilibrium flavor dynamics during the cosmic confinement transition
KFKI-1988-60/M M. Törő	The analysis of the data link layer protocol LAPB (in Hungarian)
KFKI-1988-61/G I. Tóth et al.	7.4% cold-leg break case on the PMK test facility with operation of the connection line between hot and cold legs (in Hungarian)
KFKI-1988-62/E V.Ju. Fedorovich et al.	Mandelshtam-Brillouin scattering studies on a Ca-doped Gadolinium-Gallium Garnet monocrystal
KFKI-1988-63/G Th. Bandurski et al.	Experimental investigation on core cooling at different cooling agent levels (in Hungarian)
KFKI-1988-64/D S. Zoletnik	Periodic disruptions in the MT-1 tokamak

Kiadja a Központi Fizikai Kutató Intézet
Felelős kiadó: Szegő Károly
Szakmai lektor: Bakos József
Nyelvi lektor: Harvey Shenker
Példányszám: 238 Törzsszám: 88-655
Készült a KFKI sokszorosító üzemében
Felelős vezető: Gonda Péter